

NUMERICAL STUDY OF NATURAL NANOFLUID-BASED COOLING OF A PROTUBERANT HEAT SOURCE WITHIN A SQUARE ENCLOSURE – PART I

Paulo Mohallem Guimarães, pauloguimaraes@unifei.edu.br

Marcelo Antônio Bretas, marcelobretas_ch@hotmail.com

Universidade Federal de Itajubá – Campus Itabira

Alex Pereira da Silva, alexamdv@unifei.edu.br

Genésio José Menon, genesiomemon@unifei.edu.br

Universidade Federal de Itajubá – Campus Itajubá

Abstract. *This work investigates a natural convection in a square enclosure with a protuberant heat source resembling electrical transformer. It is a laminar and non-steady regime. Finite element method is used to approximate solutions. Linear quadrilateral elements are employed to spatially discretize the domain. Several validations are carried out with numerical and experimental results. Water-based nanofluids have Copper, Alumina and Titanium oxide as its nanoparticles, separately. Lateral vertical cold walls have variable heights and they are referred to fins, which could be considered to be part of the cooling system to refrigerate electrical transformers, for example. Ten heights are studied for these cold walls. Rayleigh number ranges from 10^3 to 10^6 and the volume fraction from 0 to 0.016, totaling 9 suspension concentrations. By combining all geometrical and physical parameters, 1080 cases are run. Just part of the temperature and velocity behavior is shown here. The concentrations are chosen to be very small, since they are in agreement with the correlations used for thermal viscosity and thermal conductivity. In a general view, nanofluids proved to smoothly enhance heat transfer as the concentration increases for the range adopted.*

Keywords: *Natural convection, nanofluid, electrical transformer, heat source*

1. INTRODUCTION

Nanofluids have been scenery of quite a number of publications for the past decade due to its importance. Wen et al. (2009) presented a critical and extensive review of nanofluids for heat transfer applications. They came to the conclusion that the scientific understanding is still limited, since that many challenges are still alive which are the formulation, practical application, controlled particle size and morphology for heat transfer applications. There are some controversies in literature that may be due to uncertainties on the content of nanofluids, not to mention the solid and fluid phases. They said that not only thermal conductivity, but also other properties such as viscosity and wettability, must be seriously considered in future research. Problems with buoyancy induced flow play an important role in a variety of engineering systems due to their applications in electronic cooling, heat exchangers, etc. Ostrach (1998) made a review on these applications. Since low thermal conductivity of conventional fluids, for instance water and oils, impairs a better heat transfer performance and is a constraint of equipment compactness, an innovative technique to help enhance heat transfer, and hence decrease the size of equipment, is the use of nanoparticles in the base fluid. Such suspension composed by a base-fluid and nanoparticles was firstly named nanofluid by Choi (1995). Some numerical and experimental works on nanofluids concern thermal conductivity (Kang et al. (2006), convective heat transfer (Maiga et al.(2005), Abu-Nada (2008), boiling heat transfer and natural convection (Xuan and Li (2000). One can find a detailed review, as also mentioned in Oztop and Abu-Nada (2008), in Putra et al.(2003), Wang et al.(2006), Xuan and Li (2000), Trisaksri and Wongwises (2007), Daungthongsuk and Wongwises(2007), and Wang and Mujumdar (2007). Aminossadati and Ghasemi (2009) studied natural convection in a square cavity with a heat source placed at the bottom insulated surface. Nanofluid was composed of water-based fluid and Copper, Silver, Alumina and Titanium oxide as for its solid particles. The authors used the nanofluid thermal conductivity for spherical nanoparticles according to Maxwell (1904) and which was also cited by other researchers such as Ho et al. (2008) and Oztop and Abu-Nada (2008) . The effective dynamic viscosity was given by Brinkman (1952). Aminossadati and Ghasemi (2009) used the volume control method as for the numerical method and the Simple algorithm to handle the pressure-velocity coupling. A 60x60 uniform grid was found to meet grid independency and CPU requirements. They studied the influence on heat transfer of volume fraction that ranged from 0 to 0.20, Rayleigh number (Ra) from 10^3 and 10^6 , and heat source size from 0.2 to 0.8, for Copper, Silver, Alumina, and Titanium dioxide nanoparticles. They found that Cu and Ag nanoparticles provided the highest cooling performance, where for low Ra, the addition of 20% of these solid particles resulted in 42.8% reduction of heat source maximum temperature. Ögüt (2009) studied numerically the heat transfer by natural convection in an inclined square enclosure with a constant flux heater placed on the left vertical wall. All walls were thermally isolated, but the right vertical one, which was cooled. The heat source length was taken as 0.25, 0.50, and 1.0 (whole wall). Ra ranged from 10^4 to 10^6 . The work presented the effect of volume concentration (0 to 0.2) for Copper,

Silver, Copper oxide, Alumina and Titanium dioxide. As for the numerical method, polynomial-based differential quadrature (PDQ) was applied. According to the author, PDQ produces accurate numerical results, small number of grid points and, thus, requires small CPU time. The effective thermal conductivity adopted was the one proposed by Yu and Choi (2003), which is a modified version of Maxwell equation for a solid-liquid mixture that includes the effect of a liquid nanolayer on the surface of a nanoparticle. He found that the presence of nanoparticles caused substantial increase in heat transfer rate. The behavior of the average Nu was nearly linear with the volume fraction. Heat transfer rate started to decrease for smaller inclination angles as source length ranged from 0.25 to 1.0. The maximum and minimum Nu's were localized at inclinations 30° and 90° , respectively. Oztop and Abu-Nada (2008) conducted a study in which there was a heater under uniform temperature in an rectangular enclosure. The heater was placed on the left vertical wall. The opposite vertical wall was cooled, being that the remaining walls were isolated. The enclosure aspect ratio and also the heater size and position on the wall were investigated. The governing equations were approximated by the finite volume approach (Patankar(1980) and Versteeg and Malalasekera). The existing nanoparticles were Copper, Alumina and Titanium dioxide for a water-based nanofluid. In general, the use of nanofluids and also the increasing volume fraction increased Nu. The effect of the heater size depended mainly on the kind of nanofluid being used. For rectangular enclosures, heat transfer was more pronounced for vertically elongated enclosures. Tiwari and Das (2007) investigated the convection behavior inside a two-sided lid-driven differentially heated cavity filled with nanofluids. The vertical moving walls were isothermal and the remaining ones isolated. Results for Richardson number (Ri) ranging from 0.1 to 10 were presented. The transport equations were numerically approximated by using the finite volume technique and the SIMPLE algorithm. Water was used as the base-fluid and mixed with copper nanoparticles in some concentrations, such as 0.0%, 8%, 16%, and 20%. The effective viscosity was the one presented by Brinkman (1952) and the effective density and heat capacitance as the ones found in Xuan and Li (2000). The effective thermal conductivity of fluid was determined by the one of Maxwell-Garnett's model for spherical-particle suspension. They presented an extensive number of graphics containing streamlines and isotherms. It was observed that nanoparticles were able to change the flow pattern from natural to forced convection regime. When the walls had ascending movement, Nu was reduced compared to the other cases from the work. For $Ri < 1$, which features forced convection, with walls moving in opposite directions, Nu enhanced significantly regardless which side moved upwards. Gosselin and Da Silva (2004) performed a study on the maximization importance of thermal performance of nanofluid flow when adequate constraints are concerned. Their main objective was to examine the heat transfer on a plate from which heat was removed by nanofluid flowing on it. The mathematical model used was the one proposed by Hamilton and Crosser (1962), Xuan and Roetzel (2000) and Brinkman (1952). An analysis of the empirical shape parameter was carried out in function of volume concentration. They showed that as long as an appropriate constraint is used, heat transfer can be optimized in terms of volume fraction. By constraining the power dissipated by friction, an optimal volume fraction can be achieved by balancing low pumping power requirement and the need for an enhanced heat transfer rate.

The objective of this work is to perform an analysis on laminar natural convective heat transfer in a square enclosure with an internal heat source. This whole set is built to resemble, approximately, a transversal section of an electrical transformer with lateral solid fins as its cooling external system. In order to simulate a fin attached to the enclosure, a cold wall with variable height is located on both vertical sides of the enclosure. Nine heights are studied for Rayleigh numbers (Ra) equal to 10^3 , 10^4 , 10^5 , 10^6 and Prandtl number (Pr) 6.2 (pure water). Copper (Cu), Alumina (Al_2O_3) and Titanium dioxide (TiO_2) are used as nanoparticles to form the nanofluids. Nine volume fractions (VF or ϕ) are considered: 0 (pure water), 0.002, 0.004, 0.006, 0.008, 0.01, 0.012, 0.014, and 0.016. By combining these variations, 1080 cases are built up to be run. The finite element method is used to approximate the conservation equations, together with the Petrov-Galerkin technique to treat the convective terms and the penalty formulation to deal with the pressure terms. A linear quadrilateral element is used to discretize the spatial domain. The code is thoroughly validated by comparing present results with the ones found in numerical and experimental works from literature. In order to verify the mesh independency, two meshes are analyzed. Afterwards, results for temperature and velocity behavior will be shown. Also, many plots of Nusselt number versus fin height, volume concentration, etc, are presented.

2. MATHEMATICAL FORMULATION

Figure 1 shows a square enclosure whose outer surfaces are considered thermally isolated (hachured part) and cooled at uniform temperature T_c (non-hachured part). As for the internal surfaces, they belong to an internal heat source whose surfaces deliver a uniform and constant heat flux q'' to the inner fluid domain. The inner fluid domain is composed by a water-based nanofluid. The nanoparticles that belong to the suspensions studied are Copper (Cu), Alumina (Al_2O_3) and Titanium dioxide (TiO_2) whose thermophysical properties are shown in table 1. This work does not consider oil, which is used in most electrical transformers. This may be considered in future works. On the right side of Fig.1, one may find the respective surfaces and their dimensionless lengths, whose dimensionless boundary conditions are given by equations (16) to (21). FH stands for fin height. It takes the values 0.1, 0.2, 0.3, 0.4, 0.5, 0.6, 0.7, 0.8, 0.9 and 1.0 (whole vertical wall). This work also intends to study the interaction among the fin heights and the heat source cooling for various Rayleigh numbers. The Rayleigh number is the product of buoyancy and viscosity forces within a fluid and Prandtl number, which describes the relationship between momentum diffusivity and thermal diffusivity. Throughout

this work, half of the geometry will be studied, since there is a symmetry line at $x=0$. This saves CPU time and, hence, enables a more refined mesh on the surfaces of interest over which the Nusselt number will be calculated.

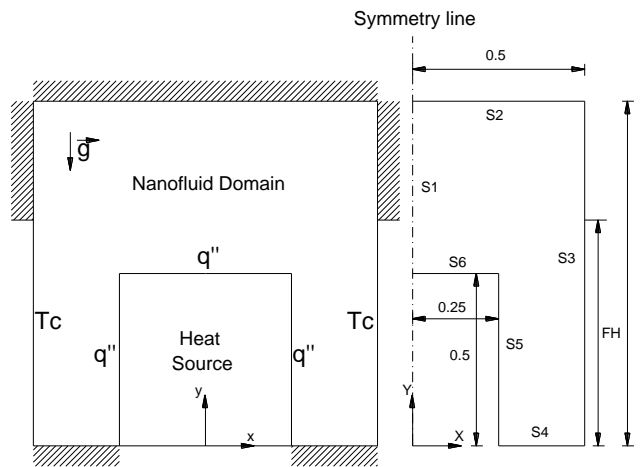


Figure 1 – Geometry and its surfaces

The governing conservation equations for the problem previously mentioned for a two-dimensional laminar and non-steady natural convection in a two-dimensional form in terms of nanofluid physical properties are given as follows:

$$\frac{\partial u}{\partial x} + \frac{\partial v}{\partial y} = 0 \quad (1)$$

$$\frac{\partial u}{\partial t} + u \frac{\partial u}{\partial x} + v \frac{\partial u}{\partial y} = \frac{1}{\rho_{nf}} \left[-\frac{\partial p}{\partial x} + \mu_{nf} \left(\frac{\partial^2 u}{\partial x^2} + \frac{\partial^2 u}{\partial y^2} \right) \right] \quad (2)$$

$$\frac{\partial v}{\partial t} + u \frac{\partial v}{\partial x} + v \frac{\partial v}{\partial y} = \frac{1}{\rho_{nf}} \left[-\frac{\partial p}{\partial y} + \mu_{nf} \left(\frac{\partial^2 v}{\partial x^2} + \frac{\partial^2 v}{\partial y^2} \right) + (\rho\beta)_{nf} g (T - T_c) \right] \quad (3)$$

$$\frac{\partial T}{\partial t} + u \frac{\partial T}{\partial x} + v \frac{\partial T}{\partial y} = \alpha_{nf} \left(\frac{\partial^2 T}{\partial x^2} + \frac{\partial^2 T}{\partial y^2} \right) \quad (4)$$

where the effective density ρ_{nf} and the thermal diffusivity α_{nf} of the nanofluid are given as:

$$\rho_{nf} = (1 - \phi) \rho_f + \phi \rho_p \quad (5)$$

$$\alpha_{nf} = k_{nf} / (\rho C_p)_{nf} \quad (6)$$

and ϕ is the solid volume fraction (*VF*) of the nanoparticles. The subscripts *f* and *p* stand for fluid and particles, respectively. The nanoparticles, which will be considered in this study, are Copper (*Cu*), Alumina (Al_2O_3), and Titanium dioxide (TiO_2). The base fluid is water with Prandtl number (*Pr*) equal to 6.2. Table 1 gives the thermophysical properties of water and nanoparticles according to Oztop and Abu-Nada (2008):

Table 1 – Thermophysical properties of fluid and nanoparticles

Physical properties	Fluid phase (water)	Cu	Al ₂ O ₃	TiO ₂
Cp (J/kgK)	4179	385	765	686.2
ρ (kg/m ³)	997.1	8933	3970	4250
K (W/mK)	0.613	400	40	30.7
β x 10 ⁻⁵ (1/K)	21	1.67	0.85	0.9

The heat capacitance $(\rho C_p)_{nf}$ and the thermal expansion $(\rho\beta)_{nf}$ of the nanofluid are written as:

$$(\rho C_p)_{nf} = (1 - \phi) (\rho C_p)_f + \phi (\rho C_p)_p \quad (7)$$

$$(\rho\beta)_{nf} = (1-\phi)(\rho\beta)_f + \phi(\rho\beta)_p \quad (8)$$

The effective dynamic viscosity μ_{nf} of the nanofluid (Brinkman (1952)) is:

$$\mu_{nf} = \frac{\mu_f}{(1-\phi)^{2.5}} \quad (9)$$

The thermal conductivity k_{nf} in Eq. (6), for spherical particles and based on Maxwell –Garnett’s model (1904), is:

$$k_{nf} = k_f \left[\frac{(k_p + 2k_f) - 2\phi(k_f - k_p)}{(k_p + 2k_f) + \phi(k_f - k_p)} \right] \quad (10)$$

where k_p is the thermal conductivity addressed to nanoparticles (Copper, Alumina and Titanium Oxide), and k_f is the thermal conductivity addressed to pure fluid (water). The Maxwell-Garnett’s model has been cited by other authors such as Aminossadati and Ghasemi (2009), Ho et al. (2008) and Oztop and Abu-Nada (2008).

Since this is a dimensionless study, Eqs. (1) to (4) should be re-written in terms of dimensionless parameters, which are as follows:

$$X = \frac{x}{L}; Y = \frac{y}{L}; U = \frac{uL}{\alpha_f}; V = \frac{vL}{\alpha_f}; P = \frac{\bar{p}L^2}{\rho_{nf}\alpha_f^2}; \tau = \frac{t}{(L^2/\alpha_f)}; \theta = \frac{(T - T_c)}{(\Delta T)}; Ra = \frac{g\beta_f L^3 \Delta T}{\nu_f \alpha_f}; \Delta T = \frac{q'' L}{k_f}; Pr = \frac{\nu_f}{\alpha_f} \quad (11)$$

For that being so, the dimensionless governing equations of mass, momentum and energy conservation are:

$$\frac{\partial U}{\partial X} + \frac{\partial V}{\partial Y} = 0 \quad (12)$$

$$\frac{\partial U}{\partial \tau} + U \frac{\partial U}{\partial X} + V \frac{\partial U}{\partial Y} = -\frac{\partial P}{\partial X} + \frac{\mu_{nf}}{\rho_{nf}\alpha_f} \left(\frac{\partial^2 U}{\partial X^2} + \frac{\partial^2 U}{\partial Y^2} \right) \quad (13)$$

$$\frac{\partial V}{\partial \tau} + U \frac{\partial V}{\partial X} + V \frac{\partial V}{\partial Y} = -\frac{\partial P}{\partial Y} + \frac{\mu_{nf}}{\rho_{nf}\alpha_f} \left(\frac{\partial^2 V}{\partial X^2} + \frac{\partial^2 V}{\partial Y^2} \right) + \frac{(\rho\beta)_{nf}}{\rho_{nf}\beta_f} Ra Pr \theta \quad (14)$$

$$\frac{\partial \theta}{\partial \tau} + U \frac{\partial \theta}{\partial X} + V \frac{\partial \theta}{\partial Y} = \frac{\alpha_{nf}}{\alpha_f} \left(\frac{\partial^2 \theta}{\partial X^2} + \frac{\partial^2 \theta}{\partial Y^2} \right) \quad (15)$$

The boundary conditions, according to Fig. 1, used to approximate a solution to Eqs. (12) to (15), are:

$$\begin{aligned} S_1 \Rightarrow U=0, \frac{\partial \theta}{\partial X}=0(\text{simmetry}); S_2 \Rightarrow U=V=0, \frac{\partial \theta}{\partial Y}=0(\text{isolated wall}) \\ S_3 \Rightarrow \begin{cases} U=V=0, \frac{\partial \theta}{\partial X}=0(\text{hachured part} \Rightarrow \text{isolated wall}) \\ U=V=0, \theta=0(\text{non-hachured part} \Rightarrow \text{cooled wall}) \end{cases} \\ S_3 \Rightarrow \begin{cases} U=V=0, \frac{\partial \theta}{\partial X}=0(\text{hachured part} \Rightarrow \text{isolated wall}) \\ U=V=0, \theta=0(\text{non-hachured part} \Rightarrow \text{cooled wall}) \end{cases} \quad S_4 \Rightarrow U=V=0, \frac{\partial \theta}{\partial Y}=0(\text{isolated wall}) \\ S_5 \Rightarrow U=V=0, \frac{\partial \theta}{\partial X}=-1(\text{wall with heat flux}); S_6 \Rightarrow U=V=0, \frac{\partial \theta}{\partial Y}=-1(\text{wall with heat flux}) \end{aligned} \quad (16)$$

The local Nusselt number on a certain surface is given by:

$$Nu_{hs}^* = \frac{hL}{k_f} \quad (17)$$

where h is the heat transfer coefficient:

$$h = \frac{q''}{T_s - T_c} \tag{18}$$

Substituting appropriate parameters from (11) and (18) into (17) yields:

$$Nu_{hs}^*(X, Y) = \frac{I}{\theta(X, Y)} \Big|_{hs} \tag{19}$$

where the subscript *hs* stands for the heater surface. The average Nusselt number is then calculated by:

$$Nu_{hs}(X, Y) = \frac{I}{0.75} \int_{hs} Nu_{hs}^* \tag{20}$$

3. NUMERICAL PROCEDURE AND CODE VALIDATION

Equations (12) to (15) are approximated by the finite element method with Petrov-Galerkin weighting on the convective terms and the pressure terms are approximated by a penalty technique with the penalty parameter equal to 10^9 . These techniques will be omitted here for a space matter. They can be found in a variety of literature, for instance, Heinrich (1999). The numerical method is implemented by using a Fortran program. The code is thoroughly validated. First validation is carried out by comparing the average Nusselt number along the hot wall, the maximum velocities in the *X* and *Y* directions and their respective positions at *Y* and *X* axes, for *Ra* equal to 10^3 , 10^4 , 10^5 and 10^6 . However, only comparisons for *Ra* equal to 10^3 and 10^6 and shown in Table 2. Air is the work fluid with *Pr* = 0.7. It consists of a benchmark problem in which a square differentially heated cavity is studied where the vertical wall temperatures are uniform and equal to 0 (cold wall) and 1 (hot wall). Excellent agreement is achieved.

Table 2. Comparison table for square differentially heated cavity with wall temperatures 0 and 1.

	Present	Khanafer et al. (2003)	Barakos and Mitsoulis (1994)	Markatos & Pericleous (1984)	De Vahl Davis (1984)	Fusegi et al. (1991)
<i>Ra</i> = 10^3						
<i>Nu</i>	1.1208	1.118	1.114	1.108	1.118	1.105
<i>U</i> _{max} (at <i>y</i> / <i>H</i>)	0.1379 (0.8120)	0.137 (0.812)	0.153 (0.806)	- (0.832)	0.136 (0.813)	0.132 (0.833)
<i>V</i> _{max} (at <i>x</i> / <i>H</i>)	0.1400 (0.1780)	0.139 (0.173)	0.155 (0.181)	- (0.168)	0.138 (0.178)	0.131 (0.200)
<i>Ra</i> = 10^6						
<i>Nu</i>	8.8363	8.826	8.806	8.754	8.799	9.012
<i>U</i> _{max} (at <i>y</i> / <i>H</i>)	0.0760 (0.8500)	0.077 (0.854)	0.077 (0.859)	- (0.872)	0.079 (0.850)	0.084 (0.856)
<i>V</i> _{max} (at <i>x</i> / <i>H</i>)	0.2620 (0.038)	0.262 (0.039)	0.262 (0.039)	- (0.038)	0.262 (0.038)	0.259 (0.033)

Second validation is shown in Fig. 2. Temperature and velocity profiles in the *y*-direction are shown for the mid-section (*Y*=0.5). The geometry and boundary conditions are the same as the ones in the first comparison. However, *Ra* is 1.89 and *Pr* is 0.71. In this case, there are some experimental results from Krane and Jessee (1983) and numerical ones from Khanafer et al. (2003). It has an excellent agreement with the numerical values and a similar behavior with the experimental ones. The third validation (not shown here) is the same benchmark problem in the previous comparisons. This time, the temperatures on the isothermal surfaces are -1 and 1, *Pr* = 0.7, and *Ra* = 10^3 , 10^4 , 10^5 . The temperature and *v*-velocity profiles are selected at *Y* = 0.5. The figures were contrasted with the ones presented in Khanafer et al. (2003) and Fidap (1990). The pictures were exactly superposed on paper and they agreed very well.

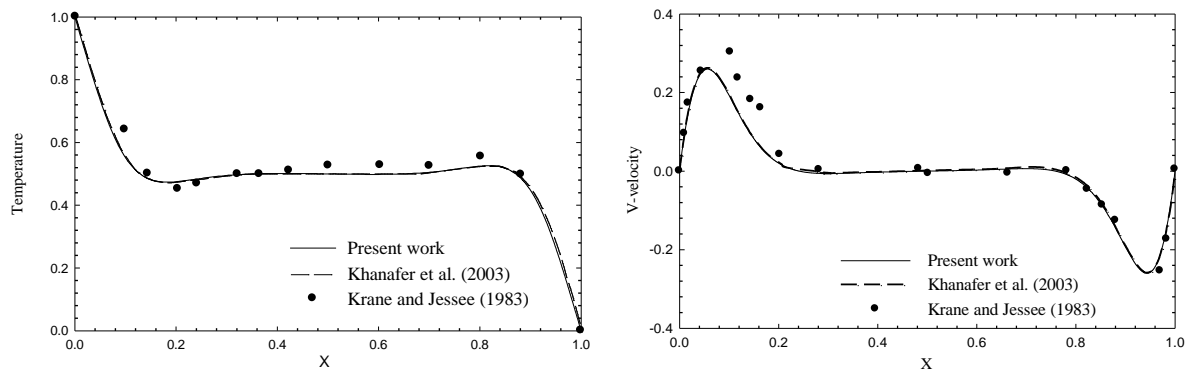


Figure 2 – Comparison of temperature velocity in *y*-direction at midsection (*Y* = 0.5) for square enclosure with differentially heated vertical walls for *Ra* = 1.89, *Pr* = 0.71.

The last validation presented here is shown in Table 3 and it is related to nanofluid behavior. The problem is taken from Aminossadati and Ghasemi (2009). The problem consists of a square cavity with a heat source with length B placed on the middle of the bottom surface. All walls are cooled at temperature zero, but the remaining bottom surface, which is isolated. The base fluid is water with $Pr = 6.2$ and the nanoparticles used are Copper, Alumina and Titanium Oxide. Results for average Nusselt number and maximum temperature on the heat source are obtained for Ra equal 10^3 , 10^4 (not shown), 10^5 (not shown) and 10^6 . In general, an excellent agreement is observed.

Table 3. Comparison for the case with a heater on the bottom of a square cavity with $\phi = 0.1$, $B = 0.4$ and $Pr = 6.2$.

		Nu _m		T _{max}	
		Present	Aminossadati and Ghasemi (2009)	Present	Aminossadati and Ghasemi (2009)
Ra=10 ³	Cu	5.4681 (0.30%)	5.451	0.205 (0.00%)	0.205
	Al ₂ O ₃	5.4075 (0.30%)	5.391	0.207 (0.00%)	0.207
	TiO ₂	5.2058 (0.32%)	5.189	0.215 (0.00%)	0.215
Ra=10 ⁶	Cu	13.5222 (2.53%)	13.864	0.109 (1.84%)	0.107
	Al ₂ O ₃	13.4093 (1.89%)	13.663	0.110 (1.82%)	0.108
	TiO ₂	13.1595 (1.95%)	13.416	0.113 (1.77%)	0.111

4. MESH INDEPENDENCY STUDY

Two grids were studied: Grid 1 and Grid 2 with 19,746 and 28, 913 quadrilateral linear elements, respectively (Table 4). A criterion for this choice is the CPU time suitable to run cases that are supposed to present results for extreme physical parameters such as $Ra = 10^3$ and 10^6 , and volume fraction 0 (pure water) and 0.4 for all nanoparticles used in this study, that is, Copper, Alumina (not shown) and Titanium dioxide (not shown). Also, FH is taken fully, that is, $FH = 1$. A special attention is given to the elements adjacent to the wall on which the average Nusselt numbers on the heat source and cold wall, Nu_{hs} and Nu_c , respectively, are going to be evaluated, since greater temperature gradients are expected there. For Grid 1, the maximum size of the element on the surface under heat flux boundary condition is 0.005 and for Grid 2, it is 0.001. The mesh quality is under the minimum angle of element internal angles, that is, elements are built by trying to set element angles as close as 90 degrees. The machine used to run all cases has 6Gb of RAM and processor Intel®Core™ 2 Duo CPU P7350 2Ghz. All these cases were run with a time step of 0.0005. The reason for this small time step for the range adopted of physical parameters is to guarantee a better convergence quality along the period of time, since a backward Euler method is used to perform time integration. In fact, a time step of 0.001 would be enough to run the cases. The convergence criterion to stop the program is:

$$Res = \frac{abs(Vel(\tau_i) - Vel(\tau_{i-1}))}{\Delta\tau} \leq 10^{-5} \tag{21}$$

where Res is the “largest velocity residual” in the entire domain in two consecutive time steps, that is:

$$\Delta\tau = \tau_i - \tau_{i-1} = 0.0005 \tag{22}$$

The velocity field lasts more than the temperature field to achieve convergence. This is why it is used in Eq. (21).

Table 4 – Grid independency study for grids 1 and 2.

Material	Ra	ϕ	Grid 1		Grid 2	
			Nu _{hs}	Tmax	Nu _{hs}	Tmax
Copper	10 ³	0	3.2952	0.3296	3.2953	0.3296
/Deviation%					0.00	0.00
Copper	10 ³	0.4	9.8399	0.1111	9.8403	0.1111
/Deviation%					0.00	0.00
Copper,	10 ⁶	0	8.2605	0.1866	8.2724	0.1865
/Deviation%					0.14	0.05
Copper	10 ⁶	0.4	10.4747	0.1111	10.4796	0.1111
/Deviation%					0.05	0.00

5. RESULTS AND DISCUSSION

Table 5 shows Nu_{hs} and θ_{max} for Water/Copper and Water/Titanium dioxide nanofluids for Ra equal to 10^3 and 10^6 , FH equal to 0.3, 0.5, and 1, and \varnothing equal to 0 and 0.01. It is clearly seen that Ra plays an important role on the heat transfer. However, the volume fraction seems to interfere just a little. Even though this is true, a more thorough study must be carried out regarding the maximum temperature that may provide interesting values when practicing practical values in temperature in Celsius degree, which is not a matter of discussion in the present work.

Table 5 – Results of Nu and θ_{max} for Copper and Titanium dioxide, $Ra = 10^3, 10^6, \varnothing = 0.0, 0.04, 0.01$.

Material	Ra	\varnothing	FH	Nu_{hs}	θ_{max}	Material	Ra	\varnothing	FH	Nu_{hs}	θ_{max}	
Copper (Cu)	10^3	0.0 (pure water)	0.3	1,9098	0,5150	Titanium dioxide (TiO ₂)	10^3	0.01	0.3	1,9568	0,5026	
			0.5	2,6688	0,3647					0.5	2,7347	0,3560
			0.7	3,1154	0,3217					0.7	3,1926	0,3139
			1.0	3,2953	0,3104					1.0	3,3771	0,3029
		0.01	0.3	1,9671	0,5000				0.3	1,9568	0,5026	
			0.5	2,7490	0,3541				0.5	2,7347	0,3560	
			0.7	3,2094	0,3123				0.7	3,1926	0,3139	
			1.0	3,3948	0,3013				1.0	3,3771	0,3029	
	10^6	0.0 (pure water)	0.3	4,1137	0,2521	10^6	0.01	0.3	4,1451	0,2498		
			0.5	6,3134	0,1528				0.5	6,3507	0,1519	
			0.7	7,5598	0,1295				0.7	7,6009	0,1287	
			1.0	8,2724	0,1191				1.0	8,3105	0,1185	
		0.01	0.3	4,1635	0,2486			0.3	4,1451	0,2498		
			0.5	6,3784	0,1512			0.5	6,3507	0,1519		
			0.7	7,6337	0,1281			0.7	7,6009	0,1287		
			1.0	8,3455	0,1180			1.0	8,3105	0,1185		

Figure 3 presents only isotherms and streamlines for $FH = 0.5$ and 1. The volume concentrations are for pure water ($\varnothing = 0$) and 0.01. It is worth mentioning that the volume concentration equal 0.001 was taken due to the correlations to be more suitable to that value. There are recirculations within the cavity which are strongly influenced by the height of the cold wall. Nevertheless, the concentration seems not to strongly modify the velocity regime, as it was expected. For height equal to 1, all the lateral vertical cooled surfaces of the cavity provide very distinguished and strong clockwise recirculations. This configuration seems to enhance heat transfer due to a longer lateral cold wall. Figure 4 depicts the Nusselt number versus the concentration for Copper for various Ra and FH . The volume concentration seems to play a more important role for cold wall heights which are shorter where the average Nusselt number on the heat source is smaller than the other cases. Then, nanoparticles would play a more important role when poor geometries are present. This is interesting because this idea may be extrapolated to other cases. However, research is still need to verify such behavior. An interesting investigation here would be the temperature on the heat source which is going to be left in a future work. Figure 5 presents the behavior of Nusselt number versus concentration. By keeping the concentration constant, Copper showed to be the best nanoparticle for all Ra and all concentrations. This was expected because Copper presents the highest thermal conductivity.

6. CONCLUSIONS

In the present work an analyses was carried out to see the influence of nanoparticles ini a base fluid (water) on the behavior of heat transfer inside a square cavity with a protuberant heat source placed inside it on the bottom surface. Many cases were seen. The Nusselt number variation was not significant when volume concentration was ranged. Nevertheless, the material played an important role when volume concentration was kept constant and a fixed Ra and a fixed fin height. The authors strongly encourage this same study with other correlations for thermophysical proportions where higher concentrations will be possible.

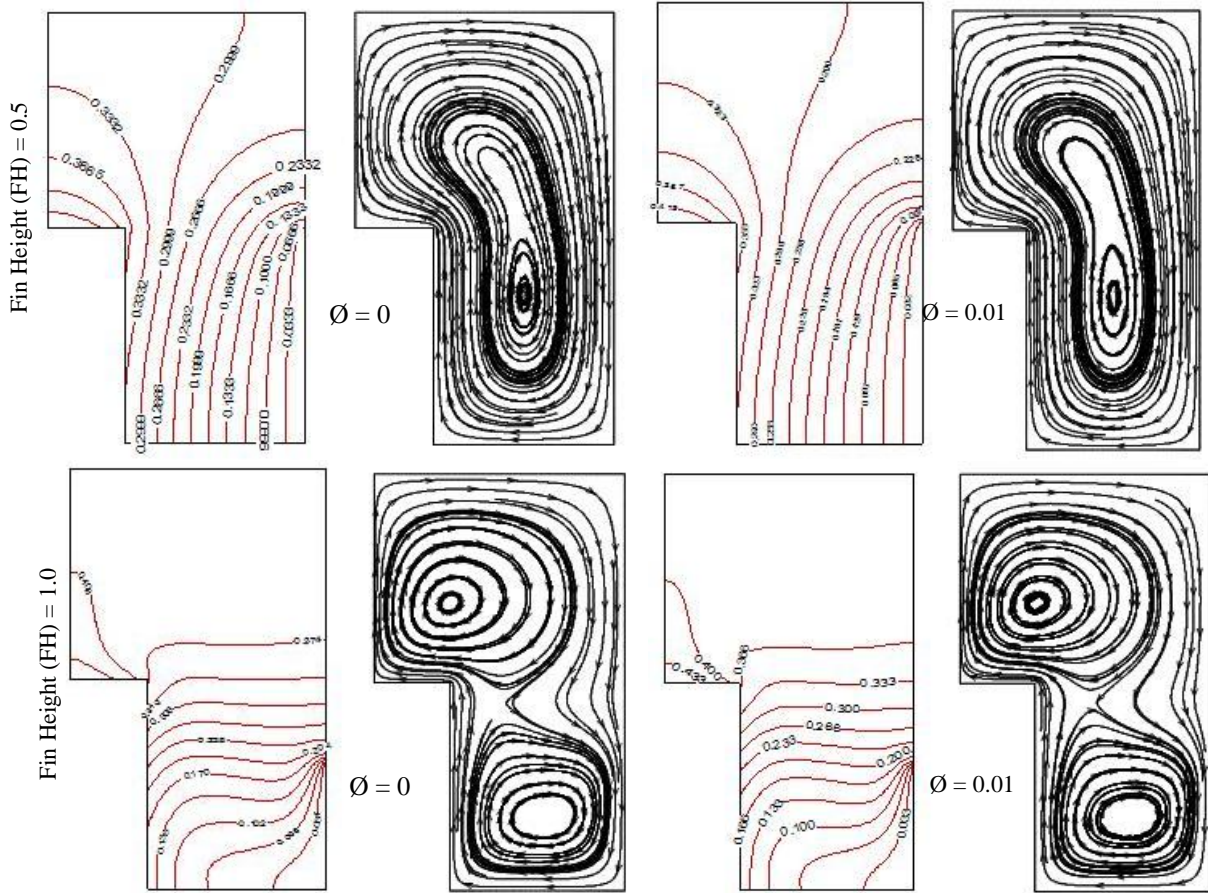


Figure 3 – Isotherms and streamlines for Copper for $Ra = 10^4$, $\varnothing = 0, 1$ and $FH = 0.3, 0.5, 0.7$ and 1.0 .

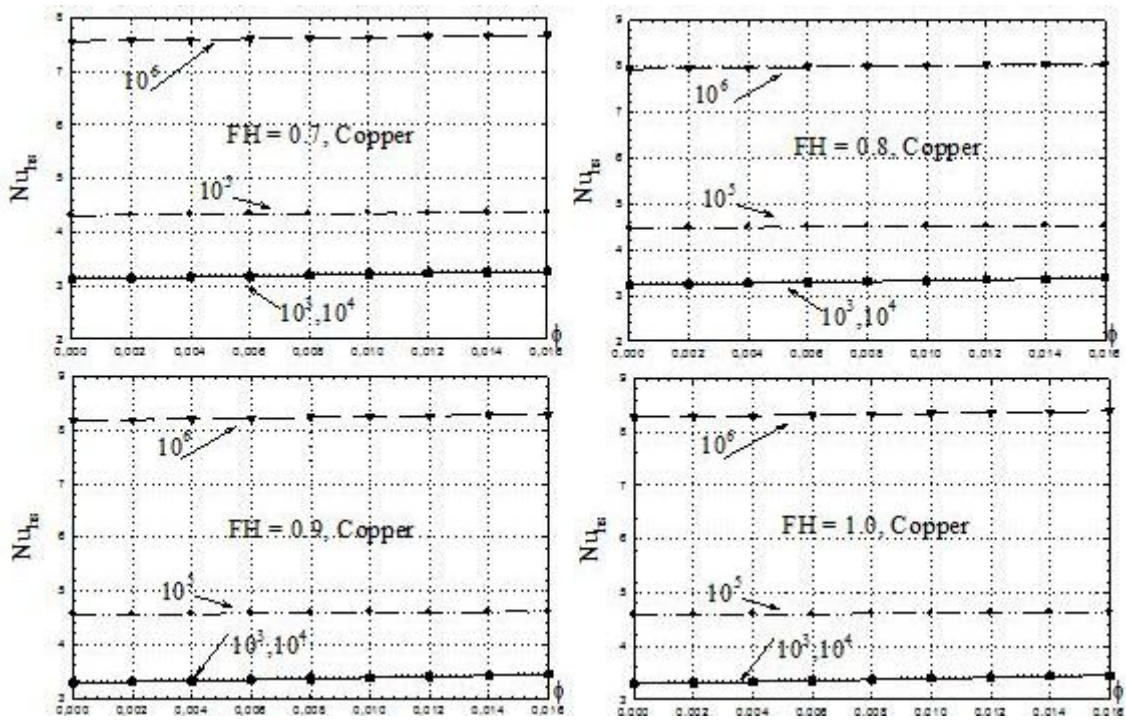


Figure 4 – $Nu_{h,s}$ versus \varnothing for Copper in all heights and Ra .

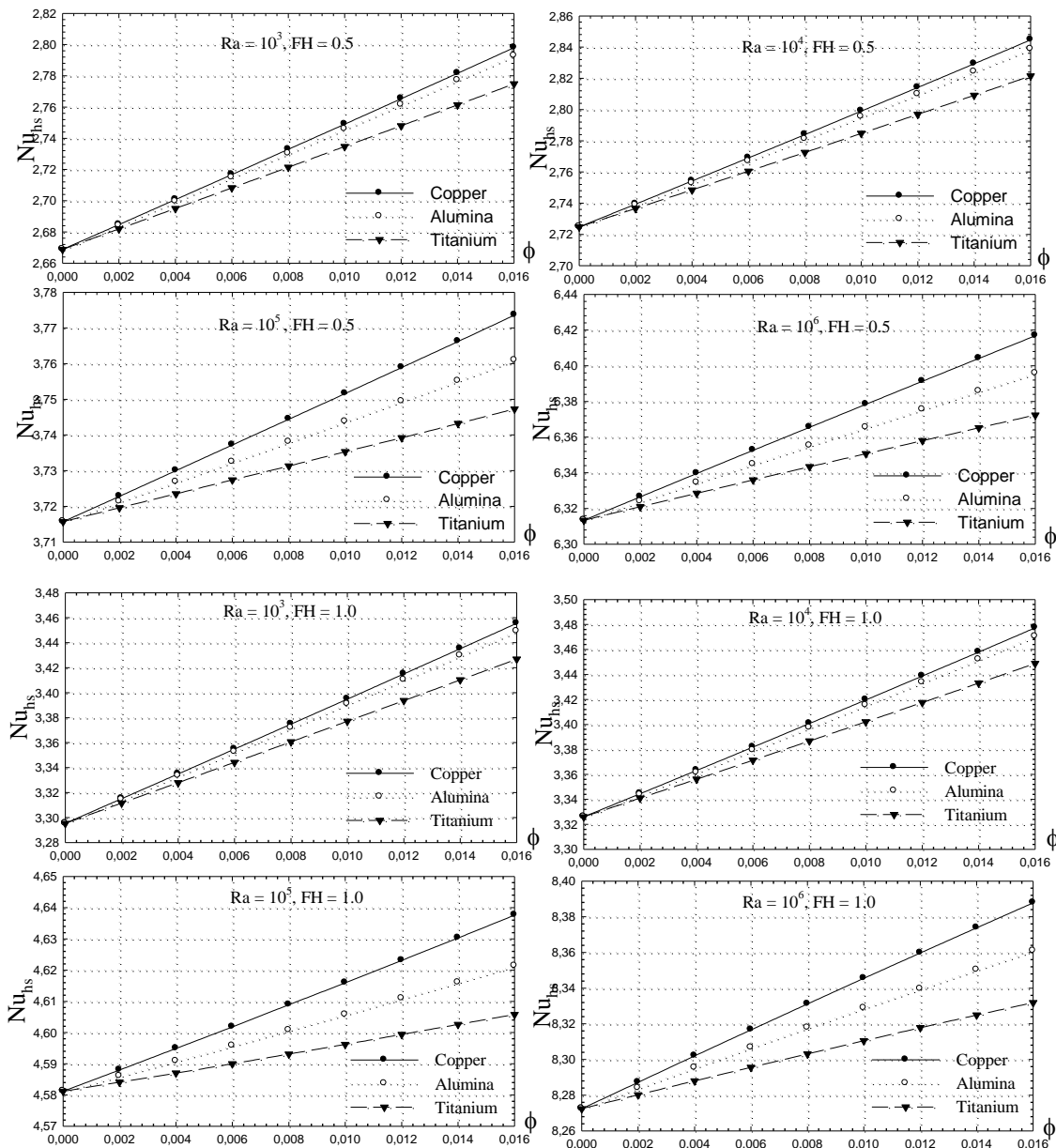


Figure 5 – Nu_{hs} versus ϕ for Copper, Alumina and Titanium for $FH = 0.5$ and 1 .

7. ACKNOWLEDGEMENTS

The authors thank CNPq and FAPEMIG for the financial support.

8. REFERENCES

- Abu-Nada E., 2008, “Application of nanofluids for heat transfer enhancements of separated flows encountered in a backward-facing step”, *Int. J. Heat Fluid Flow* 29, pp. 242-249.
- Aminossadati S.M., Ghasemi B., 2009, “Natural, convection cooling of a localized heat source at the bottom of a nanofluid-filled enclosure”, *European Journal of Mechanics B/Fluids*, pp. 1-11.
- Barakos G., Mitsoulis E., 1994, “Natural convection flow in a square cavity revisited: laminar and turbulent models with wall functions”, *Int. J. Num. Methods Fluids* 18, pp. 695-719.
- Brinkman H. C., 1952, “The viscosity of concentrated suspensions and solution”, *J. Chem. Phys.* 20, pp. 571-581.
- Choi U. S., 1995, “Enhancing thermal conductivity of fluids with nanoparticles”, in: D.A. Siginer, H.P. Wang, (Eds), *Developments and applications of Newtonian flows*, FED 231 (66), pp. 99-105.
- Daungthongsuk W., Wongwises S., 2007, “A critical review of convective heat transfer nanofluids”, *Renew Sustain. Energy Rev* 11, pp. 797-817.

- De Val Davis G., 1962, "Natural convection of air in a square cavity, a benchmark numerical solution", *Int. J. Num. Methods Fluids* 3, pp. 249-264.
- FIDAP Theoretical Manual, 1990, Fluid Dynamics International, Evanston, IL, USA.
- Fusegi T., Hyun J. M., Kuwahara K., Farouk B., 1991, "A numerical study of three-dimensional natural convection in a differentially heated cubical enclosure", *Int. J. Heat Mass Transfer* 34, pp. 1543-1557.
- Gosselin L., Da Silva A. K., 2004, "Combined "heat transfer and power dissipation" optimization of nanofluid flows", *Applied Physics Letters* 85 (18), pp. 4160-4162.
- Hamilton R. L., Crosser O. K., 1962, "Thermal conductivity of heterogeneous two-component systems", *I & EC Fundam.* 1, pp. 182-191.
- Heinrich J. C., Pepper D. W., 1999, *Intermediate Finite Element Method*, Ed. Taylor & Francis, USA.
- Ho C. J., Chen M. W., Li Z. W., 2008, "Numerical simulation of natural convection of nanofluid in a square enclosure: effects due to uncertainties of viscosity and thermal conductivity", *Int. J. Heat Mass Transfer* 51 (17-18), pp. 4506-4516.
- Kang H. U., Kim S. H., Oh J. M., 2006, "Estimation of thermal conductivity of nanofluid using experimental effective particle volume, *Exp Heat Transfer*" 19, pp. 181-191.
- Khanafer K., Vafai K., Lightstone M., 2003, "Buoyancy-driven heat transfer enhancement in a two-dimensional enclosure utilizing nanofluids", *Int. J. Heat Mass Transfer* 46, pp. 3639-3653.
- Krane R. J., Jessee J., 1983, "Some detailed field measurements for a natural convection flow in a vertical square enclosure", *Proceedings of the First ASME-JSME Thermal Engineering Joint Conference* 1, pp. 323-329.
- Maiga S. E. B., Palm S. J., Nguyen C. T., Roy G., Galanis N., 2005, "Heat transfer enhancement by using nanofluids in forced convection flows", *Int. J. Heat Fluid Flow* 26, pp. 530-546.
- Markatos N. C., Pericleous K. A., 1984, "Laminar and turbulent natural convection in an enclosed cavity", *Int. J. Heat Mass Transfer* 27, pp. 772-775.
- Maxwell J., *A treatise on electricity and magnetism*, second ed. Oxford University Press, Cambridge, UK (1904).
- Ögüt E. B., 2009, "Natural convection of water-based nanofluids in an inclined enclosure with a heat source", *Int. J. of Thermal Sciences*, pp. 1-11.
- Ostrach S., 1998, *Natural convection in enclosures*, *J Heat Transfer* 110, pp. 1175-1190.
- Oztop H. F., Abu-Nada E., 2008, "Numerical study of natural convection in partially heated rectangular enclosures filled with nanofluids", *Int. J. heat Fluid Flow*, 29 (5), pp. 1326-1336.
- Patankar S. V., 1980, *Numerical heat transfer and fluid flow*, Hemisphere Publishing Corporation, Taylor and Francis Group, New York.
- Putra N., Roetzel W., Das S. K., 2003, "Natural convection of nano-fluids", *Heat Mass Transfer* 39, pp. 775-784.
- Tiwari R. K., Das M. K., 2007, "Heat transfer augmentation in a two-sided lid-driven differentially heated square cavity utilizing nanofluids", 50, pp. 2002-2018.
- Trisaksri V., Wongwises S., 2007, "Critical review of heat transfer characteristics of nanofluids", *Renew. Sustain. Energy Rev.* 11, pp. 512-523.
- Versteeg H. K., Malalasekera W., *An introduction to computational fluid dynamic: The finite volume method*. John Wiley & Sons Inc., New York.
- Wang X.-Q., Mujumdar A. S., Yap C., 2006, "Free convection heat transfer in horizontal and vertical rectangular cavities filled with nanofluids", *Int. Heat Transfer Conference IHTC 13* Sydney, Australia.
- Wang X-Q, Mujumdar A. S., 2007, "Heat transfer characteristics of nanofluids: a review", *Int. J. Therm. Sci.* 46, pp. 1-19.
- Wen D., Lin G., Vafaei S., Zhang K., 2009, "Review of nanofluids for heat transfer applications", *Particuology*, 7, 141-150.
- Xuan Y., Li Q., 2000, "Heat transfer enhancement of nanofluids", *Int. J. Heat Fluid Flow* 21, pp. 58-64.
- Xuan Y., Roetzel W., 2000, "Conceptions for heat transfer correlation of nanofluids", *Int. J. Heat Mass Transfer* 43, pp. 3701-3707.
- Yu W., Choi S.U.S., 2003, "The role of interfacial layers in the enhanced thermal conductivity of nanofluids: a renovated Maxwell model", *J. Nanoparticle Res.* 5, pp. 167-171.

9. RESPONSIBILITY NOTICE

The authors are the only responsible for the printed material included in this paper.